Journal of Mines, Metals and Fuels, *73(2): 321-332; 2025. DOI: 10.18311/jmmf/2025/46413*

Print ISSN : 0022-2755

Journal of Mines, Metals and Fuels

Contents available at: *www.informaticsjournals.co.in/index.php/jmmf*

Effect of Process Parameters in Submerged Friction Stir Welding to Improve the Corrosion Resistance of Aluminum Alloy (AA7075)-Experimental and Mathematical Approach

Levi P. Cheworei[1]*, D. Balaji Naik[2], M. Yaswanth Kumar Reddy[3], K. Srinivasa Rao[4] and G. Rambabu[1]

[1]Mechanical Department, Andhra University, Vishakapatnam – 530003, Andhra Pradesh, India; levizcheworei@gmail.com

[2]AI Engineering Services Limited, Dum Dum, Kolkata – 700051, West Bengal, India

[3]Mechanical Department, Andhra University, Vishakapatnam – 530003, Andhra Pradesh, India

[4]Metallurgical Engineering, Andhra University, Vishakapatnam – 530003, Andhra Pradesh, India

Abstract

The present work pertains to an experimental and mathematical approach to the optimisation of the corrosion properties of AA7075-T6 Aluminum alloy welds. Friction Stir Welding (FSW) in a submerged water condition, was carried out on a vertical lathe machine to make a welded joint of aluminium alloy while the process parameters were varied to determine a combination that gives an optimum condition with improved corrosion resistance. The process parameters, namely tool rotational speed (rpm), transverse speed (mm/min) and axial force (kN) have a pivotal role in determining the microstructural and corrosion resistance in the welded joint region. The work is to develop a mathematical model that can be referenced as an optimum corrosion resistance property of a submerged friction stir welded aluminium alloy AA7075-T6 joint through optimisation of process parameters. The experimental data was statistically analysed and the response surface methodology approach enabled the development of the optimised mathematical model that predicts the optimised corrosion resistance of AA7075. The Minitab software was used to obtain a mathematical model that is used to predict the optimum corrosion resistance of AA7075 and optimised values. Finally, the significance of the developed mathematical model was tested through the Analysis of Variance (ANOVA), which showed that tool rotational speed has a great influence on the corrosion resistance rate of the submerged friction stir welded joint.

Major Findings: *1. The corrosion resistance decreases with an increase in the tool rotational speed and welding speed. 2. The submerged friction stir welded joint has better corrosion resistance properties when compared to joints made on base metal. 3. A mathematical regression model that predicts the corrosion resistance of SFSW joint, an AA7075 aluminium alloy joint, was developed with a confidence level of above 95%.*

Keywords: *Aluminum Alloy AA7075, Corrosion Resistance, Process Parameters, Response Surface Methodology (RSM), Submerged Friction Stir Welding.*

**Author for correspondence*

1.0 Introduction

The 7xxx aluminium alloy series contains aluminium, zinc, magnesium and copper (Al-Zn-Mg-Cu) as its main components. Zinc (Zn) is approximately 5-6 %, Magnesium (Mg) 2-3 % and copper (1.5%). Aluminium alloy AA7075 has other metallic elements in small quantities, such as chromium (Cr), Manganese (Mn) and Titanium (Ti). $MgZn_2$ precipitated in AA 7075 Aluminum alloy helps to harden the joint structure and improves the mechanical properties when subject to heat treatment[1]. AA7075 is mostly preferred as a structural material owing to its high specific strength-to-weight ratio, good corrosion resistance and easy workability. Its high specific strength, and lightweight to natural ageing combination make it applicable in areas such as the automobile industry, aerospace industries and shipping industries[2]. The FSW is a technique that is relatively new for joining metals and alloys that was invented at The Welding Institute (TWI) of England in the year 1991. It's solid-state welding of metals and alloys using a hard abutting non-consumable rotating welding tool mounted on the welding machine. Conventional welding has been a common practice in joining metals whereby metals are welded together by applying heat with a filler that, over time, has demonstrated disadvantages like strength and easy corrosion of the joint that needs to be improved. Aluminum metal is a soft, light and reactive metal that in its pure form possesses low metal strength but its mechanical properties increase when alloyed. However, its corrosion resistance tends to reduce exposure to higher temperatures for long periods. In FSW submerged in water condition, the tool consists of a tool pin, which adopts different geometry that may include square, hexagonal, triangle and pentagon or cone shape and the shoulder. Its purposes are; one, generate heat. When the welding tool rotates, the friction between the rotating tool and the base material being joined produces a lot of heat and this causes the abutting zone of the base material to soften, hence making it easy for fabrication to take place. Two, the shoulder controls the hot material flow along the welding zone from spilling to avoid material wastage and three, ensures the defect-free joint is produced by ensuring grain compactness. The tool geometry has a great influence on the joint quality. An extensive profile study on the influence of tool pin geometry on aluminium alloy welds reports that a hexagonal profile tool gives superior mechanical properties when compared to other tool profiles. Also, ANOVA has been used to determine the adequacy of the model developed and evaluate the statistical significance of evaluate quadratic model, including the coefficient of correlation (R2)[3]. The rotating tool stirs and softens material along the welded part of the plates, leading to the formation of three frictional heat-affected zones depending on the magnitude of the heat. The zones formed are the Nugget Zone (NZ), also called the Stir Zone (SZ), the Thermo-Mechanically Affected Zone (TMAZ) and the Heat Affected Zone (HAZ). When the welding tool is rotating while traversing in the welding direction, it leads to materials transfer from the backside of the pin to the front side and the materials from the advancing side to the retreating of the pin[4-6]. Increasing the welding speed during the friction stir welding process leads to changes in the crystalline arrangement at the thermos-mechanically affected zone and changes in the material grain size of the welded joint. This indicates the role the welding speed and the welding tool pin geometry play during joint formation through friction stir welding[7]. The mechanical properties of the welded joint are superior when compared to joints formed by conventional welding methods. The thermal cycle during FSW affects the mechanical properties of the welded joint, because of microstructural changes that cause strength in the TMAZ and the HAZ of the joint. Notably, the presence of precipitates is responsible for the strength of the parent metal and weld joint of the aluminium alloy. The depreciation or coarsening of the precipitate causes poor mechanical properties of the joint. When joining thick aluminium alloys of 6mm and above thickness, there is thermal variation in the longitudinal direction due to the high thermal conductivity of aluminium alloy and this forms uniform aluminium alloy material. To remedy such deformities caused by heat generated during welding in the thermo-mechanical affected zone and heat affected zone, the effects of water cooling on the performance of friction stir the welding process on the heat-affected zones in that a coolant has to be introduced to bring the cooling effect to the welding zone and that will increase the weld joint strength. The coolant can be water or nanofluid. Water as a cooling agent is comparatively more efficient than nano fluid because of its high heat transfer coefficient and uniform cooling effect[8-25]. A research study on friction

stirs weld of AA2219-T6 aluminium alloy with water as a medium in a submerged condition reported a superior joint formed in terms of corrosion, attributed to the effect of limiting dissolution and coarsening of the precipitate that affects the joint strength. Further, it investigated and established an improvement in the corrosion rate of the water-submerged friction stir welded joint of AA7075-T87 aluminium alloy by minimising the heat-affected zone width[26-33]. Extensive studies have been conducted on friction stir welding. Unfortunately, there is little literature on temperatures submerged friction stir welding where welding temperatures are controlled, welding parameters are varied to various levels and optimised to achieve an improved corrosion property of AA7075 aluminium alloy. Additionally, variables that determine the metal and alloy joint microstructure and properties as a result of plastic deformation and material stir during the welding process stirring as the shoulder diameter and tool pin length have not been widely studied.

2.0 Experimental Design

2.1 Material and Methods

In this work, AA7075-T6 aluminium alloy plate experiments 300mm x 300mm x 7mm thickness (Figure 1(a)) were used to make weld joints when carrying out SFSW experiments. For the plates in water-submerged condition, a single welding pass was done on each plate using a wear-resistant, non-consumable hexagonal tapered tool pin profile (Figure 1(b)) fixed onto a horizontal welding machine (Figure 1(c)), with a constant water head of 35mm supply as coolant running through to the welding pass. The aluminium alloy chemical properties are indicated in Table 1.

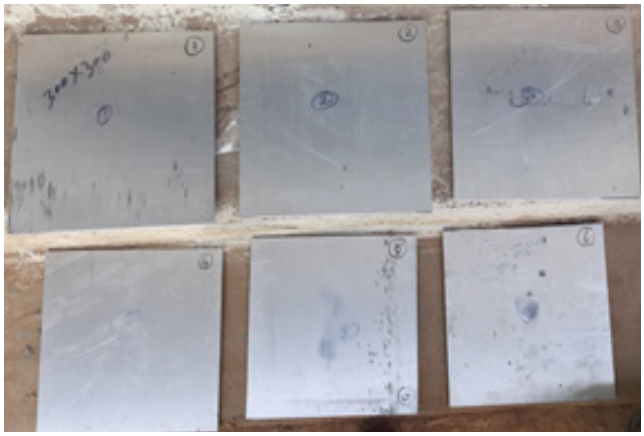


Figure 1(a). Sample base material of AA 7075 alloy.



Figure 1(b). Hexagonal tapered welding tools.



Figure 1(c). Welding machine for SFSW.



Figure 1(d). Submerged friction stir welded result.

Table 1. Chemical composition of AA 7075 alloy

Element	Al	Zn	Mg	Cu	Si	Others
wt. %	89.25	5.5	2.5	1.6	0.2	Bal

2.2 Corrosion Test

Potentio-dynamic polarization test was carried out to find the corrosion characteristics of AA7075 alloy using ASTM B117, ISO 9227 machine coupled with salt spays on the material during the tests which were conducted with salty spays concentrated at 3.5% sodium chloride solution. The potential scan current increased suddenly and was taken to be the critical corrosion potential. The joint with a less negative result indicates a better corrosion-resistant joint.

2.3 Design of Experiments

It's hard to develop a regression model that can predict the optimum corrosion resistance rate of materials that generally possess a high rate of corrosion resistance. To remedy this, the study employed critical process parameters that affect the process of developing a submerged friction stir welded joint that enhances its corrosion resistance. Table 2 below is a design of an experiment showing process parameters with their levels which were independently varied as specified in the preliminary experiments. Due to the array of parameters that can influence the corrosion resistance of AA7075, a decision to employ three parameters and five levels with a central composite design which helped to dictate the total number of experiments to be conducted as shown in Table 3 was made. A tapered hexagonal pin profile is used across all levels.

2.4 Development of a Mathematical Model for Corrosion Resistance

Optimising corrosion resistance in AA7075 alloy aims at improving a general mechanical property of the alloy metal, corrosion resistance is taken as a function of the process parameters.

$$CR=f(N,S,F) \quad (1)$$

The corrosion resistance model with 2nd order regression model used to represent the surface response is expressed as,

$$CR = m + \sum m_i y_1 + \sum m_{ii} y_2 + \cdots + \sum m_n y_n \quad (2)$$

For the three process parameters involved in this work with factors interaction, the corrosion polynomial regression model equation is given as;

$$CR = m_0 + m_1(N) + m_2(S) + m_3(F) + m_{11}(N_2) + m_{22}(S_2) + m_{33}(F_2) + m_{12}(NS) + m_{13}(NF) + m_{23}(SF) \quad (3)$$

Where m_o, is the average of the responses and $m_1, m_2, m_3 \ldots\ldots m_{23}$ are coefficients that depend on the respective interaction effects of the factors. The coefficients were tested for their significance at a 95% confidence level using a Minitab software 2017 package.

Table 2. Process parameters and their levels.

S/N	Process Parameter	Denotation	Unit	Level				
				-1.68	-1	0	+1	+1.68
1	Rotational Speed	N	RPM	500	600	700	800	900
2	Welding Speed	S	MM/MIN	100	110	120	130	140
3	Axial Force	F	kN	4	5	6	7	8

Table 3. The experimental results for the corrosion design matrix.

Experiment Number	Factors Coded Values			Factors Actual Values			Corrosion Rate E_{pit}/(mV)
	Tool Rotational Speed (N)	Welding Speed (S)	Axial Force (F)	N	S	F	
1	0	0	0	700	120	6	-547
2	0	1.68	0	700	160	6	-565
3	0	0	0	700	120	6	-548
4	0	-1.68	0	700	80	6	-570
5	1	-1	-1	800	100	5	-565
6	0	0	0	700	120	6	-549
7	1	-1	1	800	100	7	-579
8	-1	-1	1	600	100	7	-559
9	0	0	0	700	120	6	-547
10	-1.68	0	0	500	120	6	-564
11	-1	1	1	600	140	7	-578
12	1	1	-1	800	140	5	-568
13	1	1	1	800	140	7	-583
14	0	0	1.68	700	120	8	-566
15	0	0	0	700	120	6	-547
16	-1	1	-1	500	140	5	-570
17	1.68	0	0	900	120	6	-605
18	0	0	-1.68	700	120	4	-560
19	0	0	0	700	120	6	-548
20	-1	-1	-1	600	100	5	-555

The experimental data of the corrosion rate of the AA7075 alloy metal in water submerged are indicated in Table 3.

The 20 experimental data shown in Table 3 are a set of coded conditions used to make the design matrix prescribed by central composite design when three parameters are chosen for study. They are the input data that is used to develop a mathematical equation that represents corrosion resistance when the design of the experiment method and Response Surface Methodology (RSM) in mini-tab software is used.

The resultant mathematical model developed in Equation 4 is to predict the rate of optimum corrosion resistance of SFSW joints of AA7075-T6 aluminium alloy and its analysis of variance is shown in Table 4.

$$CR = \begin{Bmatrix} -547.78 - 7.47N - 2.39S + 3.74F - 12.28N^2 \\ -6.27S^2 - 4.68F^2 + 3.37NS - 2.13NF + 0.62SF \end{Bmatrix} \quad (4)$$

From Table 4 above, the analysis of variance for corrosion result shows the value of tool rotational speed (N) in the linear model to be 0.002 which is less than

Table 4. Analysis of Variance for corrosion

Source	DF	Adj SS	Adj MS	F-Value	P-Value
Model	9	3839.68	426.63	9.68	0.001
Linear	**3**	**1030.03**	**343.34**	**7.79**	**0.006**
N	1	761.12	761.12	17.26	0.002
S	1	77.78	77.78	1.76	0.214
F	1	191.13	191.13	4.34	0.064
Square	**3**	**2679.27**	**893.09**	**20.26**	**0.000**
N*N	1	2174.79	2174.79	49.33	0.000
S*S	1	567.29	567.29	12.87	0.005
F*F	1	316.06	316.06	7.17	0.023
2-Way Interaction	**3**	**130.37**	**43.46**	**0.99**	**0.438**
N*S	1	91.12	91.12	2.07	0.181
N*F	1	36.13	36.13	0.82	0.387
S*F	1	3.12	3.12	0.07	0.795
Error	**10**	**440.47**	44.09		
Lack-of-Fit	5	437.54	87.51	131.26	0.000
Pure Error	5	3.33	0.67		
Total	19	4280.55			

Model Summary

S	R-sq	R-sq(adj)	R-sq(pred)
6.63982	89.70%	80.43%	22.24%

0.05 (95% confidence level). This indicates that the tool rotational speed had the most influence over the rest of the parameters. Axial force (F) with a value of 0.064 was the second most influencing and welding speed last effective parameter of SFSW with a value of 0.214. The determinant coefficient (R^2) is used to indicate how close the predicted model and experimental value lie[34]. In this work, the determinant coefficient (R^2) is 89.7% showing that 10.3% of the variation is not explained by the model. Implying that there is a high correlation between the predicted values and the experimental values. The corrosion rate normal probability graph in Figure 3 shows the residual fall on a straight line, implying that the errors are normally distributed. This points to the goodness of the regression model developed.

3.0 Optimisation of Process Parameters

The multi-objective simulation approach with mixed model sequencing was used to find the optimum values of the process parameters[34]. The factor's coded values are used to develop a mathematical model which is optimised and converted to actual experimental values.

Maximize Corrosion resistance $(CR) = f(N, S, F)$

$-1.68 \leq CR \geq 1.68$

Table 5. Optimised CR submerged friction stir weld factors

S/n	Parameters	Optimized VHN Values	Corrosion Rate (mV)
1	Tool rotational speed (N)-rpm	700	545.72
2	Tool advancing speed (S)-mm/min	120	
3	Axial force (F)-kN	6.4	

Parameters Range

$-1.68 \leq N \geq 1.68$

$-1.68 \leq S \geq 1.68$

$-1.68 \leq F \geq 1.68$

From the model, the optimised values of the corrosion rate are indicated in Table 5.

4.0 Results and Discussion

When the SFSW process takes place, high temperatures are achieved due to frictional heat. Plastic deformation that occurs in the process leads to the formation of the recrystallised microstructure at the welding zone. When the welding bead is pressed against AA7075 material being joined, the weld nuggets are formed due to the penetration of the welding tool and this causes an "onion ring" effect in the direction where the tool is advancing. The welding process extrudes a semi-cylinder layer of material that has a similar appearance to an onion ring structure when viewed on a cross-section. The measured section of a weld nugget of the hexagonal tool was 21mm. The high temperatures and plastic deformation determine the mechanical properties in the welded zone and the extent to which plastic deformation occurs determines

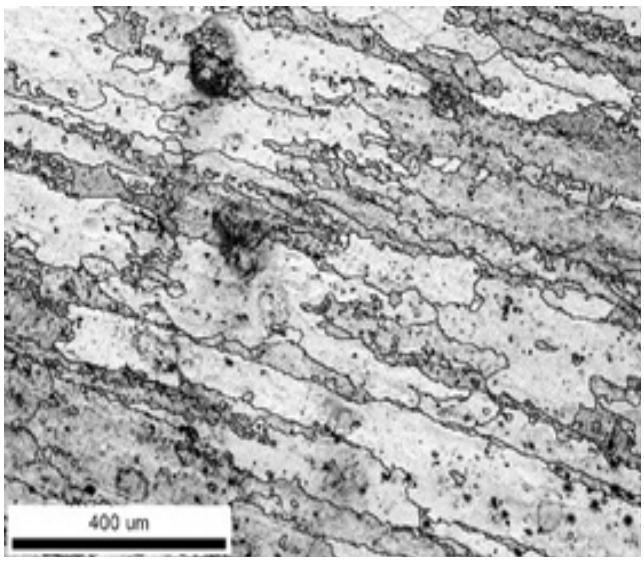


Figure 2(a). Base metal in a 400μm scale.

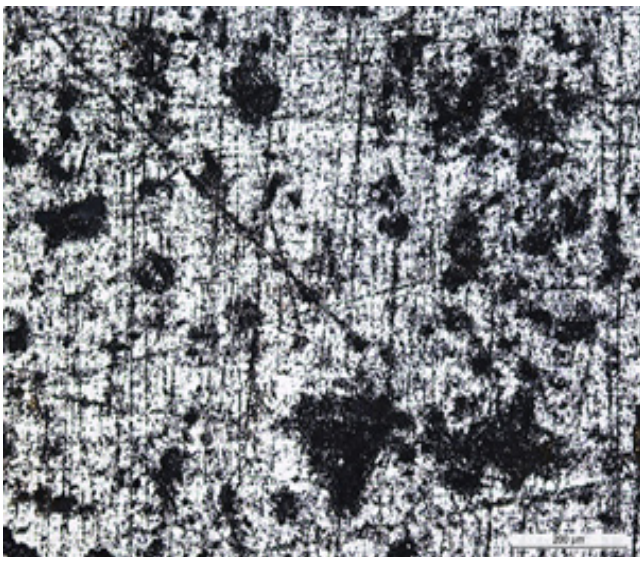


Figure 2(b). Submerged FSW in a 200μm scale.

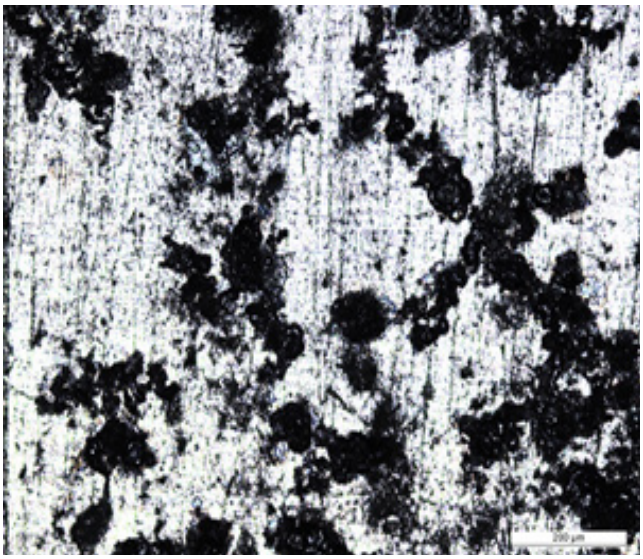


Figure 2(c). Normal FSW in a 200μm scale.

the microstructure of the joint. The submerged water condition resulted in the formation of a fine grain structure at the weld zone with smaller grain sizes observed (Figure 2(b)) than base metal (Figure 2(a)) and normal FSW joints as illustrated in Figure 2(c). This is due to dynamic recrystallisation that is evenly distributed as a result of the regulated welding temperatures, a key element in determining the level of corrosion resistance in aluminium alloy (AA7075) metal.

The pitting corrosion of the weld nugget of AA7075 is by the local dissolution of components of the material elements making the alloy. The relative positivity of the Epit value in the nugget zone of the SFSW is due to the coarsening of the strengthening precipitate that is formed at the weld joint. Experimental results of corrosion resistance indicate that the joint formed with process parameters of a tool rotational speed of 700 rpm, welding speed of 120 mm/min and an axial force of 6 kN in water-submerged condition registered superior corrosion resistance, which was more positive in the reader compared to other joints.

4.1 Normality Test

The normal probability plot for the data is a straight line indicating the normal distribution of errors, thus justifying the suitability of the regression model. In this study, the optimum corrosion resistance of a submerged stir welded joint was Epit of -545.72 mV with a rotational speed of 700rpm, welding speed of 120mm/min and an axial force of 6.4kN.

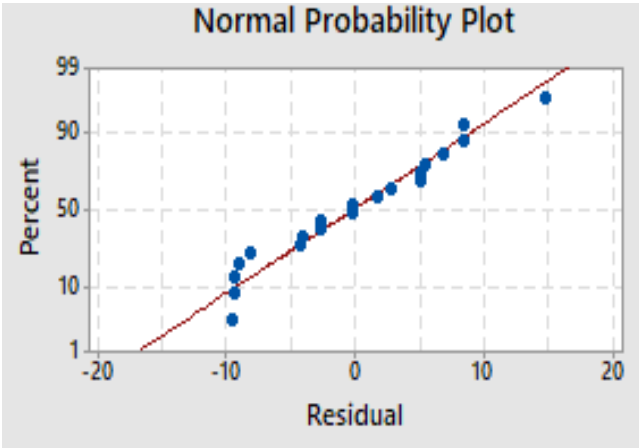


Figure 3. CR normality test graph.

4.2 Analysis of the Contour and Response Surface Plots

4.2.1 Contours Plots

The contour plots in Figure 4(a)-(c) give a clear distinction of the corrosion rates at different levels as it is sensitive to smaller changes in the process parameters. The circular contour plots, Figures 4(a) and 4(c)) are an indication of the independence of factors involved in rotational speed and welding speed.

Corrosion resistance is more sensitive to axial force and welding speed interaction as indicated in Figure 4(b). The corrosion resistance is more positive at a combination of high-level axial force and low-level welding speed.

From contour plots, it's inferred that the elliptical nature of the contour plots indicates that there is an interaction of process factors during the submerged welding process of AA7075 as shown in Figure 4b. From the figure, the axial force and advancing speed had more impact on the SFSW process. The corrosion rate is more sensitive at optimum axial force speed and welding speed. The corrosion rate is maximum from the plots when the optimised values are; tool rotational speed is 700rpm, welding speed 120mm/min and axial force is at 6.4kN.

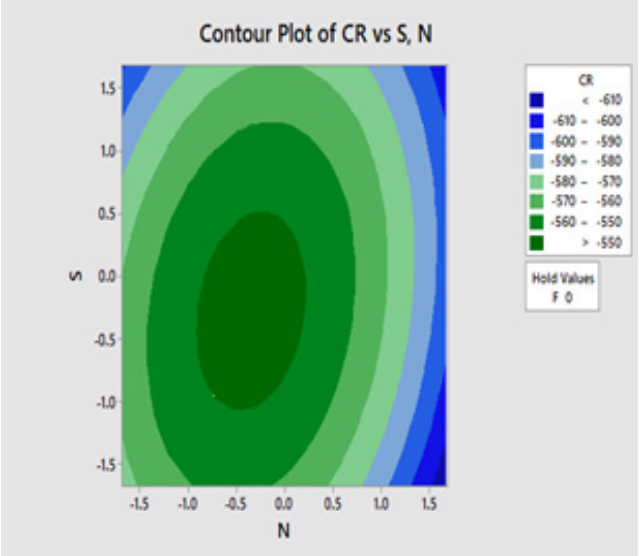


Figure 4(a). Circular nature of contours implying affect tool rotation speed and welding speed on corrosion are independent during SFSW.

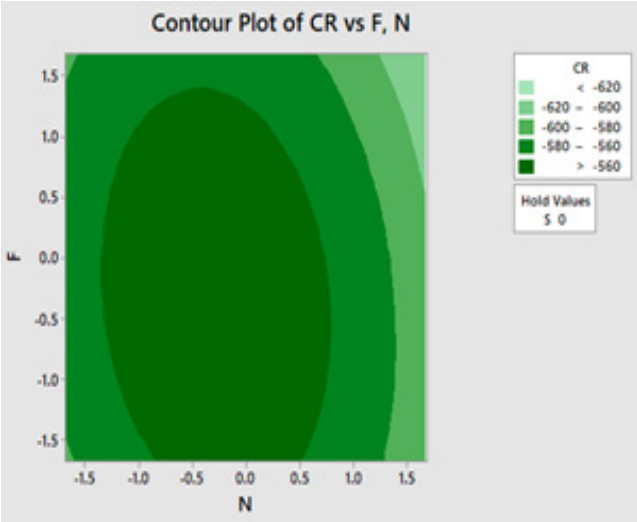


Figure 4(b). Elliptical nature of contours implying interaction of rotational speed and axial force on corrosion during SFSW.

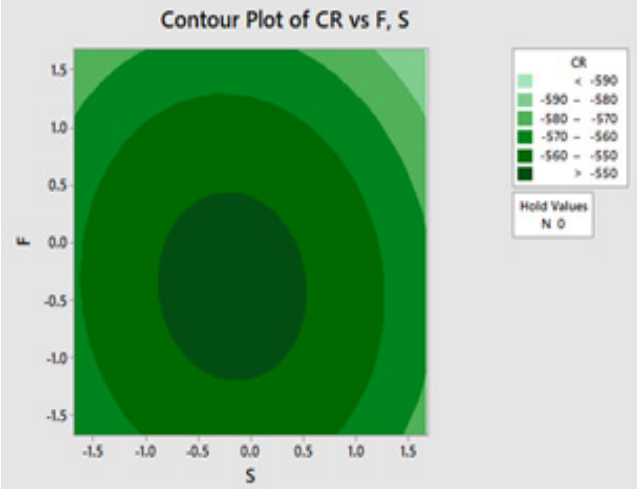


Figure 4(c). Circular nature of contour implying axial force and welding speed on corrosion are independent during SFSW.

4.2.2 Response Surface Plots

Graphs below Figure 5(a-c) is a three dimension corrosion resistance-responsive surface plots from the developed regression model. The maximum point of the response surface indicates the optimum corrosion resistance rate.

In terms of individual parameters, corrosion resistance is more sensitive to changes in welding speed than changes in tool rotational speed. The parameters' interaction effect between welding speed and axial force on the corrosion rate manifests itself as indicated in Figure 5(c). The corrosion rate is more positive at low-level welding speed and high-level axial force.

4.3 Effect of Tool Rotational Speed

SFSW joints that were formed at a minimum rotational speed of 500rpm and a maximum speed of 900rpm both registered lower corrosion properties when compared against the joints made from other levels as shown in

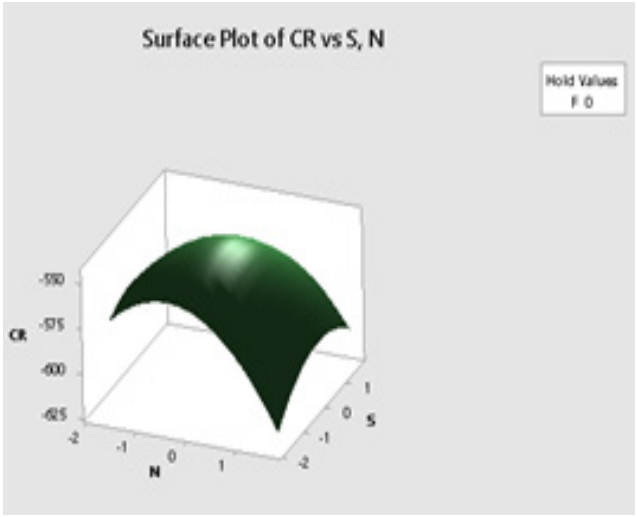


Figure 5(a). Corrosion is sensitive at low tool rotational speed and high welding speed.

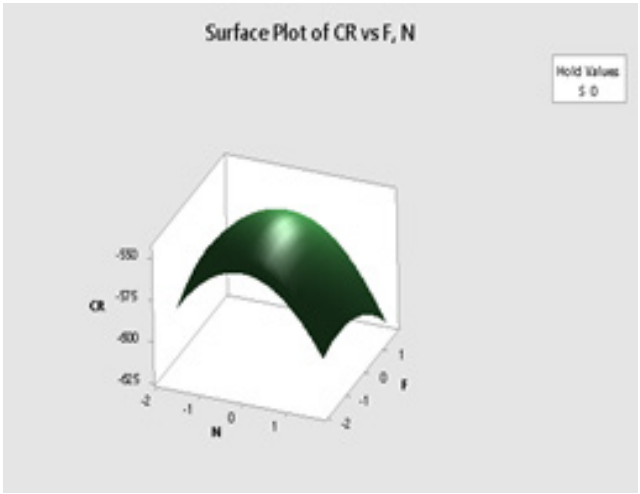


Figure 5(b). Corrosion is sensitive at low level rotational speed and low axial force.

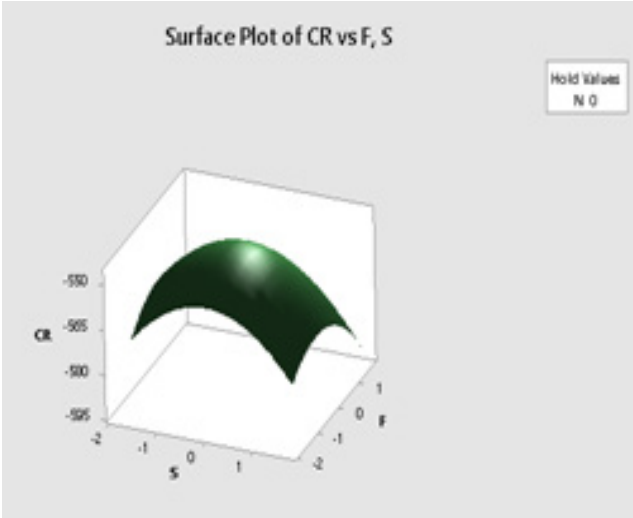


Figure 5(c). Corrosion is more sensitive at low welding speed and mid-level axial force.

Table 3. The corrosion rates registered at this level were -513mV and -511mV respectively.

4.4 Effect of Welding Speed

The SFSW joint made at a welding speed of 80mm/min exhibited a superior corrosion rate of -516mV compared to joints made from the levels in the welding process. This means that when the welding speed of the joint is formed in a submerged condition, a low welding speed is preferable for a better joint to be made, as the result indicates a more positive corrosion rate value than other joints at different levels of the welding process.

4.5 Effect of Axial Force

The corrosion rate at an axial force of 6kN registers a higher positive corrosion rate of -516 mV compared to the other axial force at different welding levels as shown in the corrosion test results. This infers that the axial force should be kept at a balancing force to obtain an optimum corrosion resistance rate of a submerged friction stir welded aluminium alloy.

4.0 Conclusion

The submerged friction stir welded joint has better corrosion resistance properties when compared to joints made on base metal and a normal condition friction stir weld joint of AA7075 aluminium alloy metal. This is attributed to the controlled welding temperature during the submerged friction stir welding that enables the joint material grain to quickly coalesce, hence avoiding the formation of the precipitate and leading to fine material grain. Hence, the rapid water cooling of the weld line during the submerged friction stir welding process leads to enhancement of the corrosion properties of the AA7075 alloy metal. The corrosion resistance decreases with an increase in the tool rotational speed and welding speed because of an increase in the heat generated during the welding process and that affects alloy microstructure formation. A mathematical model that predicts the corrosion resistance of a submerged friction stir welded joint, an AA7075 aluminium alloy joint, was developed with a confidence level of above 95%. It involved the process parameters and statistical tools such as regression analysis and design of experiments. The optimised values had a close relation to the experimented data. The interaction effect of process parameters was evident in AA7075 as illustrated by the contour plots response graphs.

5.0 Acknowledgment

The authors extend the greatest gratitude to the Andhra University Department of Metallurgical Engineering, Visakhapatnam Andhra Pradesh, India for providing insight and advice on materials to conduct this research. Thankful to Sri Venkateshwara Industries, Balanagar Hyderabad, India for allowing submerged friction stir welding experiments in their establishment.

6.0 References

1. Prasanna P. Effect of tool pin profile and heat treatment process in the friction stir welding of AA6061 aluminium alloys. Am J Eng Res. (AJER). 2013; 2(1):7-15.
2. Nandan R, Debroy T, Bhadeshia H. Recent advances in friction stir welding process, welding structure and properties. Prog Mater Sci. 2008; 53(6):980-1023. https://doi.org/10.1016/j.pmatsci.2008.05.001
3. Rambabu G, Naik BD. Optimization of friction stir welding parameters for improved corrosion resistance of AA2219 aluminium alloy joints. Def Technol. 2015; 11(4):330-337. https://doi.org/10.1016/j.dt.2015.05.003

4. Fujii H, Kato H, Nakata K, Nogi K. Friction stir welding. Proc 6th Int Symp. TWI. Saint- Sauveur, Montreal, Canada; 2006.
5. Fujji L, Cui, Maeda M, Nogi K Effect of tool shape on mechanical properties and microstructure of friction stir welded aluminium alloys. Mater Sci Eng. A. 2006; 419(1-2):25-31. https://doi.org/10.1016/j.msea.2005.11.045
6. Jata KV, Sankaran KK, Ruschau JJ. Friction stir welding effects on microstructure and fatigue of aluminium alloy AA7075-T6". Metallurgical and Material Transaction A. 2000; 31(9):2181-2193. https://doi.org/10.1007/s11661-000-0136-9
7. Saliha G, Mouloud A, Fouad B, Younes B. Design and optimization of friction stir welding tool. Weld Technol. 2010; 25(11):1199-1205. https://doi.org/10.1080/10426910903536733
8. Zhang HJ, Liu HJ. Effect of water cooling on the performances of friction stir welding heat-affected zone. J Mater Eng Perform. JMEPEG. 2010; 21(7):1182-1187. https://doi.org/10.1007/s11665-011-0060-8
9. Mehta K. Advanced joining and welding techniques: An overview. In: Gupta, K, editor. Advanced manufacturing technologies. Materials Forming. Machining and Tribology. Springer, Cham; 2017. https://doi.org/10.1007/978-3-319-56099-1_5 PMCid: PMC5615874.
10. Jayaraman, M, Sivasubramanian R, Balasubramanian V, Lakshminarayanan AK. Optimization of process parameters for friction stir welding of cast aluminium alloyA319 by Taguchi Method. J Sci Ind Res. 2009; 68(1):36-43.
11. Davim PJ, Gupta K. Advanced manufacturing, advanced welding and deforming. Elsevier. 2021. p. 1-22.
12. Venkatesha BN. Preliminary studies on mechanical and metallurgical behaviour of friction stir welded butt joints. Procedia Eng. 2014; 97:847-853. https://doi.org/10.1016/j.proeng.2014.12.359
13. Li JQ, Liu HJ. Optimization of welding parameters for the reverse dual rotation friction stir welding of a high-strength aluminium alloy 2219-T6. Int J Adv Manuf Technol. 2014; 6(5-8):1469-1478. https://doi.org/10.1007/s00170-014-6352-z
14. Davim JP. Statistical and computational techniques in manufacturing, Springer; 2012. Available from: https://link.springer.com/book/10.1007/978-3-642-25859-6
15. Rathinasuriyan C, Senthil Kumar VS. Experimental investigation of weld characteristics on submerged friction stir welded 6061-T6 aluminium alloy. J Mater Sci Technol. 2017; 31(8):3925-3933. https://doi.org/10.1007/s12206-017-0738-4
16. Sucharitha M, Ravi Sankar B, Rao PU, Experimental investigation on the effect of tool rotational speed on mechanical properties and microstructure of friction stir welded AZ31 Mg alloy. Mater Today: Proceeding. 2021; 46(9):3455-3459. https://doi.org/10.1016/j.matpr.2020.11.788
17. El-Moayed M. Shash H, Rabou AY, El-Sherbiny MG. A detailed process design for conventional friction stir welding of aluminium alloys and an overview of related knowledge. Eng Rep. 2020; 3(2):1-17. https://doi.org/10.1002/eng2.12270
18. Elangovan K, Balasubramanian V, Valliappan M. Influences of tool pin profile and axial force on the formation of friction stir processing zone in AA6061 aluminium alloy. Int J Adv Manuf Technol. 2008; 38(3):285-295. https://doi.org/10.1007/s00170-007-1100-2
19. Fratini L, Buffa G, Shivpuri R. Mechanical and metallurgical effects of in-process cooling during friction stir welding of AA7075-T6 butt joints. Acta Mater. 2010; 58(6):2056-2067. https://doi.org/10.1016/j.actamat.2009.11.048
20. Davim PJ. Perceptions of Industry 5.0: Sustainability perspective. Bio Res. 2025; 20(1):15-16. https://doi.org/10.15376/biores.20.1.15-16
21. Srinivasan PB, Arora KS, Dietzel W, Pandey S. Schaper MK. Characterization of microstructure, mechanical properties and corrosion behavior of an AA2219 friction stir welded. J Alloys Compd. 2009; 492(1-2):631-637. https://doi.org/10.1016/j.jallcom.2009.11.198
22. Palanivel R, Koshy PM. Prediction and optimization of process parameter of friction stir welded AA5083-H111 Aluminum alloy using response surface methodology. J Cent South Univ. 2012; 19(1):1-8. https://doi.org/10.1007/s11771-012-0964-y
23. Elatharasan G. An experimental analysis and optimization of process parameters on friction stir welding of AA 6061-T6 aluminium alloy using RSM. Procedia Eng. 2013; 64:1227-1234. https://doi.org/10.1016/j.proeng.2013.09.202
24. Kadaganchi R, Gankidi MR, Gokhale H. Optimization of process parameters of aluminium alloy AA2014-T6 friction stir welds by response surface methodology. Defence Technol. 2015;11:209-219. https://doi.org/10.1016/j.dt.2015.03.003
25. Dhanapal A, Boopathy RS, Balasubramanian V, Chidambaram K, Thoheer Zaman AR. Experimental

investigation of the corrosion behaviour of friction stir welded AZ61A magnesium alloy welds under salty spray corrosion test and galvanic corrosion test using response surface methodology. Int J Met. 2013; 1-17. https://doi.org/10.1155/2013/317143

26. Kesharwani RK. Multi-objective optimization of friction stir welding parameters for joining of two dissimilar thin aluminium sheets. Procedia Mater Sci. 2014; 6:178-187. https://doi.org/10.1016/j.mspro.2014.07.022
27. Davim JP. Manufacturing: A bibliometric analysis. Int J Manuf Mater Mech Eng. 2024;13(1). https://doi.org/10.4018/IJMMME.360710
28. Zhang HJ, Liu HJ, Yu L. Microstructure and mechanical properties as function of rotation speed in underwater friction stir welded aluminium alloy joint. Mater Des. 2011; 2:442-4407. https://doi.org/10.1016/j.matdes.2011.03.073
29. Wang Q, Zhao Y, Yan K, Lu S. Corrosion behavior of spray formed 7055 aluminium alloy joint welded by underwater friction stir welding. J Mater Des. 2015; 68:97-103. https://doi.org/10.1016/j.matdes.2014.12.019
30. Santhanam SKV, Ramaiyan S, Rathinaraj L, Chandran R. Optimization of parameters: Tool pin profile, rotational speed and welding speed for submerged friction stir welding od AA6063 alloy. Int J Tech Res Appl. 2016; 35-38.
31. Seung-Ju Sun. Influence of friction stir welding on mechanical properties of butt joints of AZ61 magnesium alloy. Adv Mater Sci Eng. 2017; 6:1-13. https://doi.org/10.1155/2017/7381403
32. Sucharitha M, Sankar BR, Rao PU. Experimental investigation on the effect of tool rotational speed on mechanical properties and microstructure of friction stir welded AZ31 Mg alloy. Mater Today: Proceeding. 2021; 46(9):3455-3459. https://doi.org/10.1016/j.matpr.2020.11.788
33. Montgomery DC. Design and analysis of experiments. New York: John Wiley and Son; 2001
34. McMullen PR, Frozier GV. A simulated annealing approach to mixed model sequencing with multiple objective. IIE Trans. 2000; 32:679-686. https://doi.org/10.1023/A:1007611509671